Scaling Laws for Dynamical Hysteresis in a Multidimensional Laser System

Angela Hohl, H. J. C. van der Linden, and Rajarshi Roy
School of Physics, Georgia Institute of Technology, Atlanta, Georgia 30332-0430

Guillermo Goldsztein, Fernando Broner, and Steven H. Strogatz*
Department of Mathematics, Massachusetts Institute of Technology, Cambridge, Massachusetts 02139
(Received 5 August 1994; revised manuscript received 14 November 1994)

We examine scaling laws for dynamical hysteresis in an optically bistable semiconductor laser. An analytic derivation of these laws from multidimensional laser equations is outlined and they are expected to be universal for systems that exhibit a cusp catastrophe. The scaling laws for the hysteresis loop area or width are numerically verified and experimentally measured for operation of the bistable laser above and below threshold. Excellent agreement with theory is obtained in the limit of low switching frequencies.

PACS numbers: 05.45.+b, 42.65.Pc

Hysteresis is ubiquitous in optical, electronic, magnetic, and mechanical switching elements, and is of great practical concern as well as of fundamental scientific interest [1–4]. In fact, it has recently been demonstrated that hysteresis is present even in the most microscopic of systems: the one-atom micromaser [5]. The extent of hysteresis, often measured by the width or area of the hysteresis loop obtained when an appropriate system variable is plotted as a function of the switching parameter, may depend on the frequency of switching and also on the operating parameters of the switching element itself. Some of the basic questions that remain to be explored are the regimes for which certain scaling laws exist and whether the exponents obtained for systems obeying diverse microscopic dynamics are valid for others.

In this Letter we examine the bistable semiconductor laser, a device that has been proposed as a basic switching element for optical systems [1,6–9]. Starting from the four-dimensional rate equations for this system, we derive scaling laws for dynamical hysteresis in the limit of low switching frequency. As described by these equations, a laser undergoes a bifurcation at threshold. We predict that the scaling exponents depend on where the bistable laser is biased with respect to threshold. The analysis suggests that the same exponents should also be valid for other multidimensional systems that exhibit a cusp catastrophe [10]. The predictions are verified numerically and experimentally; the scaling exponents determined for operation both above and below threshold are in excellent agreement with theoretical predictions.

In the experimental system (Fig. 1) a single mode laser field is injected close to resonance into a laser diode which is biased around threshold. The strength of the external injected field E_{ext} is varied sinusoidally. The output of the bistable laser then exhibits bistability and hysteresis. Dagenais *et al.* have experimentally characterized the adiabatic (or quasistatic) bistable behavior and hysteresis in a similar system as a function of detuning between the injected field and a mode of the bistable semiconductor laser, as well as of the operating point of the laser with respect to threshold [6].

The dynamics of such a laser system is described by the rate equations [7,8]

$$\dot{\mathcal{E}} = \frac{1}{2}\left[G_n\Gamma(N - N_t) - \frac{1}{\tau_p}\right]\mathcal{E} - i(\omega_2 - \omega_1)\mathcal{E} - \kappa E_{\text{ext}},$$

$$\dot{S} = \left[G_n\Gamma(N - N_t) - \frac{1}{\tau_p}\right]S + \frac{C_{\text{sp}}N}{\tau_s},$$

$$\dot{N} = \frac{I}{q} - \frac{N}{\tau_s} - G_n(N - N_t)(|\mathcal{E}|^2 + S),$$

$$(\omega_2 - \omega_1) = \frac{n_{\text{eff}}}{n}\Delta\omega_0 - \frac{1}{2}\alpha G_n\Gamma(N - N_0), \qquad (1)$$

where $\mathcal{E}$ is the complex amplitude of the internal single mode electric field, N is the carrier number, and S is the average photon number generated by spontaneous emission into the lasing mode. Spontaneous emission is necessary to describe laser operation below threshold and is incorporated deterministically to facilitate the analytic derivation outlined below. Alternatively, the influence of

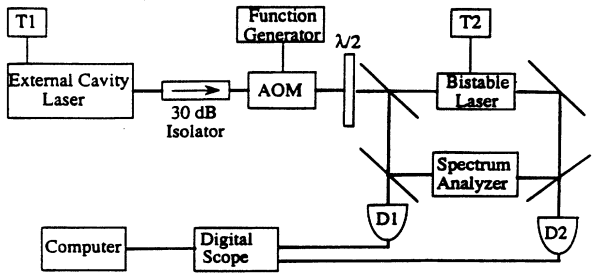

FIG. 1. Experimental setup of the bistable semiconductor laser system with modulated external input. $T1$ and $T2$ are temperature controllers, AOM is the acousto-optic modulator, and $D1$ and $D2$ are photodetectors.

 0031-9007/95/74(12)/2220(4)$06.00

spontaneous emission could be accounted for through stochastic Langevin noise terms in the equation for $\mathcal{E}$ and N. The incident external electric field amplitude E_{ext} is assumed to be of the form $E_{\text{ext}} = E\sin\Omega t$. The detuning between the injected signal and the time-dependent laser frequency is given by $\omega_2 - \omega_1$, and $\Delta\omega_0$ is the fixed detuning between the frequencies of the external field and the solitary laser. Because of this detuning the observed hysteresis is primarily dispersive in nature and is related to a change in the effective index of refraction of the gain medium. N_0 is the steady state carrier number when the external field is zero and is obtained by solving (1) with the time derivatives set to zero. It is a function of the injection current I, and, of the two possible solutions for N_0, the one corresponding to the stable fixed point is selected. Table I lists the meaning and typical values of the other parameters.

It is found that when E_{ext} is changed adiabatically, hysteresis is observed in the laser intensity $P_{\text{tot}} = |\mathcal{E}|^2 + S$ vs the injected intensity $|E_{\text{ext}}|^2$, when I is above a critical value. For the purpose of the theoretical analysis, this critical value is defined to be the threshold current I_{th}. In the graph of P_{tot} vs $|E_{\text{ext}}|^2$ we examine the hysteresis loop area as a function of the switching frequency Ω for different bias currents I close the I_{th}.

We predict that for sufficiently small Ω, the dynamical hysteresis area A is given by

$$A(\Omega) = A_0 + C\Omega^{\beta}, \tag{2}$$

where the static area $A_0 \neq 0$ if and only if $I > I_{\text{th}}$, and β is given by

$$\beta = \begin{cases} 1 & \text{for } I < I_{\text{th}}, \\ \frac{4}{5} & \text{for } I = I_{\text{th}}, \\ \frac{2}{3} & \text{for } I > I_{\text{th}}. \end{cases} \tag{3}$$

Our analysis [11] shows that the scaling exponents in (3) are universal for dynamical systems in which bistability arises as a parameter crosses a phase transition point. More precisely, (3) holds whenever one stable equilibrium point splits into three (two stable, one unstable) via the generic mathematical mechanism called a cusp catastrophe [10].

TABLE I. Value of parameters.

τ_p	1.4×10^{-12} s	Photon lifetime
κ	1.3×10^{11} s^{-1}	Coupling constant
τ_s	10^{-9} s	Carrier lifetime
G_n	1.93×10^{4} s^{-1}	Differential gain
Γ	0.15	Confinement factor
α	3	Linewidth enhancement factor
C_{sp}	10^{-5}	Spontaneous emission coupling ratio
n	3.5	Refractive index
n_{eff}	4.1	Effective index
N_t	1.33×10^{8}	Transparency carrier number
$\Delta\omega_0$	-14 GHz	Fixed detuning

We now outline the derivation of $\beta = \frac{4}{5}$ for $I = I_{\text{th}}$; this is the most delicate case. The first step is a center manifold reduction of the full dynamics, which yields a reduced equation of the form

$$\dot{x} = -cx^3 + E\sin\Omega t, \tag{4}$$

where $c > 0$. Let $T = 2\pi/\Omega$. For small Ω, there exists a T-periodic, locally stable solution of (4), which we denote $z(t)$. Using a quasistatic approximation, one expects $z(t) \approx x_0(t)$, where $cx_0(t)^3 = E\sin\Omega t$. Let $z(t) = x_0(t) + u(t)$. Inserting $z(t)$ in (4) and making the approximations $|u| \ll |x_0|$ and $|\dot{u}| \ll |\dot{x}_0|$, we find $u(t) \approx -\dot{x}_0/3cx_0^2$ and hence

$$u(t) \approx \frac{-\Omega\cos\Omega t}{9(Ec^2)^{1/3}(\sin\Omega t)^{4/3}}. \tag{5}$$

Equation (5) can be used to show that the original assumptions $|u| \ll |x_0|$ and $|\dot{u}| \ll |\dot{x}_0|$ are self-consistent if $\Omega \ll \Omega_0 \equiv 3(E^2c)^{1/3}$ and $\sin\Omega t$ and $\cos\Omega t$ are not too close to 0. To state the conditions precisely, let k be a constant such that $1 \ll k \ll (\Omega_0/\Omega)^{3/5}$ and let $\tau_0(\Omega) \equiv k(E^2\Omega^2c)^{-1/5}$. Let $\tau_1(\Omega)$ be defined such that $(cE^2)^{-1/3} \ll T/4 - \tau_1 \ll T$. Then we find [11] that (5) is valid for $\tau_0 \leq t \leq \tau_1$, where we have restricted attention to the quarter cycle $0 \leq t \leq T/4$; by symmetry, (5) is valid on corresponding parts of the other quarter cycles.

Next we calculate the area of the hysteresis loop [12] defined by the plane curve $(E\sin\Omega t, z(t))$. The area is $A(\Omega) = |E\Omega\int_0^T z(t)\cos\Omega t\,dt|$. Substitute $z(t) = x_0(t) + u(t)$ and observe that the integral involving $x_0(t)$ vanishes because there is no static hysteresis for (4). Hence $A(\Omega) = |E\Omega\int_0^T u(t)\cos\Omega t\,dt|$. Let $A_1(\Omega)$ denote the part of the integral that comes from the intervals where (5) is valid, and let $A_2(\Omega)$ denote the remaining part. Then substitution of (5) into the integral yields

$$A_1(\Omega) \approx \frac{4E\Omega^2}{9(Ec^2)^{1/3}}\int_{\tau_0}^{\tau_1}\frac{\cos^2\Omega t}{(\sin\Omega t)^{4/3}}\,dt. \tag{6}$$

The dominant contribution to this integral comes from the neighborhood of the lower limit, where $\sin\Omega t$ is small and the integrand is large. To see this, note that $\Omega\tau_0 = k(3\Omega/\Omega_0)^{3/5} \ll 1$, where the inequality follows from the definition of k. Furthermore, $\pi/2 - \Omega\tau_1 \ll 1$, from the definition of τ_1. Evaluating the integral to leading order in Ω, we find

$$A_1(\Omega) \approx \frac{4E^{4/5}}{3k^{1/3}c^{3/5}}\Omega^{4/5}. \tag{7}$$

The remaining area $A_2(\Omega)$ cannot be calculated accurately, since the approximation for $u(t)$ breaks down, but $A_2(\Omega)$ can be proven to be bounded above by a quantity which is itself of order $O(c^{-3/5}E^{4/5}\Omega^{4/5})$. Thus $A(\Omega)$ is strictly $O(\Omega^{4/5})$ for small Ω, since it is bounded both above and below by quantities of this order.

For $I < I_{\text{th}}$, the scaling law $A(\Omega) \sim \Omega$ is derived by techniques similar to those above, but the analysis

is more straightforward and can be carried out in a multidimensional setting [11]; there is no need for a center manifold reduction. For $I > I_{th}$, the result $A(\Omega) \sim \Omega^{2/3}$ follows from an extension of the techniques in [13]. There, the scaling exponent of $\frac{2}{3}$ was obtained for the one-dimensional equation $\dot{x} = ax - bx^3 + E\sin\Omega t$, with $a, b > 0$.

Numerical simulations of (1) were done to verify the predicted scaling laws. The results are shown in Fig. 2, where β is plotted as a function of the bias current of the laser with respect to threshold. The exponent changes from $\beta \approx 1$ below threshold to $\beta \approx 0.6$ above threshold. The computations are extremely time consuming in the low-frequency limit, since the time scales involved in the equations range from picoseconds to tens of milliseconds. The results shown in Fig. 2 are estimates of the exponents obtained. The systematic errors are due to the difficulty of accessing the extreme low-frequency limit. It should be noted that the equation for spontaneously emitted photons contributes dominantly below the solitary laser threshold. Furthermore, the contribution of spontaneous emission to P_{tot} is significant around threshold but is not needed to produce static hysteresis above threshold.

In the experiments (Fig. 1) the injected field was obtained from a single frequency external cavity semiconductor laser system. The bistable laser, and HLP 1400 Fabry-Pérot diode with wavelength $\lambda \approx 830$ nm, was temperature stabilized to better than 0.01 K and an optical isolator prevented feedback into the external cavity laser. A function generator was used with an acousto-optic modulator to sinusoidally vary the externally injected signal. A half-wave plate insured that the polarization of the injected signal matched that of the bistable laser. The spectrum of the output from the bistable laser was monitored on an optical spectrum analyzer. The injected signal intensity and the output intensity of the bistable laser were detected using two fast photodiodes and recorded on a digital oscilloscope interfaced to a computer.

We focused on measurements above and below threshold, since it is extremely difficult to determine the laser threshold precisely and maintain the laser at that point. Figure 3(a) shows data for above threshold operation ($I/I_{th} = 1.08$). We note that the definition of threshold used in the experiments differs slightly from the one mentioned above [14]. The half-widths H are determined from measurements of many hysteresis loops, and are used instead of loop areas since the loop height remains constant. H_0, measured for a modulation frequency $\nu = 10$ Hz, is taken as a good approximation to the half-width of the static hysteresis loop. A log-log plot of the low-frequency measurements is used to estimate the scaling exponent as follows. Values of $\ln(H - H_0)$ from the lowest frequency to a chosen Ω_{max} are plotted versus $\ln(\Omega)$, as shown in Fig. 3(b), and an estimate of the scaling exponent is obtained from a linear regression fit to the data. Then, the highest-frequency point for the plot is omitted, and the scaling exponent estimate is obtained from the rest of the points. This procedure is followed until the number of points in the plot is too small for a reasonable linear fit. The results are shown in Fig. 3(c), from which we estimate $\beta = 0.62$ in the low-frequency limit. The data for operation below threshold ($I/I_{th} = 0.94$) are plotted in Fig. 4(a). The width of the loop at the lowest frequency of modulation (10 Hz) is much smaller than that for above threshold operation. In this case the low-frequency observations [Fig. 4(b)] indicate that $\beta = 1.01$.

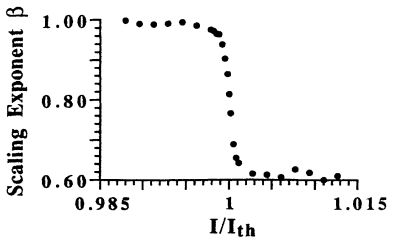

FIG. 2. Numerically calculated scaling exponent β as a function of the normalized bias current I/I_{th}.

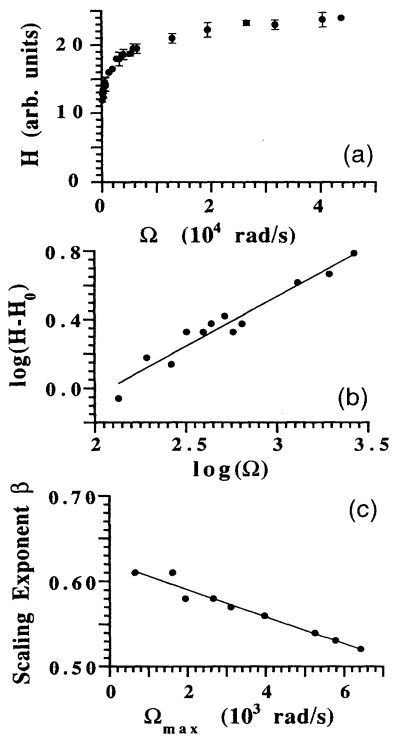

FIG. 3. Experimental results for the half-width of the hysteresis loop where the laser is pumped above threshold ($I/I_{th} = 1.08$). (a) Half-width of hysteresis loop as a function of modulation frequency. (b) Estimation of the scaling exponent β by linear regression. (c) Determination of the low-frequency limit for β.

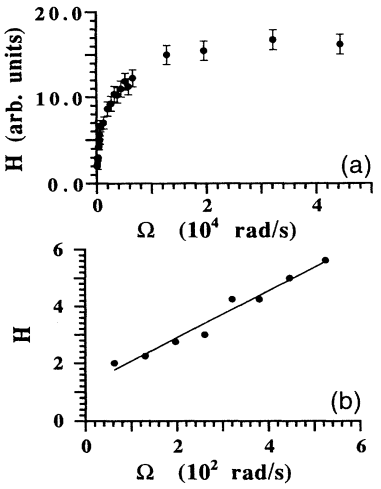

FIG. 4. Experimental results for the half-width of the hysteresis loop where the laser is pumped below threshold ($I/I_{th} = 0.94$). (a) Half-width of hysteresis loop as a function of modulation frequency. (b) Linear regression fit to low-frequency data.

For higher frequencies (but not so high as to distort the hysteresis loop), the scaling laws break down. This intermediate regime extends over many orders of magnitude of the switching frequency and further theoretical studies need to be done to gain insight into the laws governing this regime.

We note that several mean-field treatments of the kinetic Ising model show a similar scaling behavior of the hysteresis loop area at low frequencies [15]. Also, the theoretical results reported here are not limited to the system (1), but are valid for any bistable system in which a cusp catastrophe occurs. Therefore these scaling laws are of a universal nature and we expect the results to be valid for other such multidimensional systems. In particular, the subthreshold scaling law $A(\Omega) \sim \Omega$ is even more general; it is valid for dynamical hysteresis about any linearly stable steady state. Noise in the dynamical system does not appear to play a significant role in the regime investigated, but its inclusion may be relevant at still lower frequencies and for other systems.

This research was supported in part by NSF Grants No. ECS-9114232, No. DMS-9057433, and No. DMS-9111497. We thank Chris Luse, Fedor Mitschke, James Sethna, and Andrew Zangwill for helpful discussions.

*Present address: Theoretical and Applied Mechanics, Cornell University, Ithaca, NY 14853.

[1] H. M. Gibbs, *Optical Bistability: Controlling Light with Light* (Academic Press, Orlando, 1985).
[2] M. A. Krasnosel'skii and A. Pokrovskii, *Systems with Hysteresis* (Springer-Verlag, Berlin, 1989).
[3] A. B. Pippard, *The Physics of Vibration* (Cambridge University Press, Cambridge, 1989).
[4] C. Boden, F. Mitschke, and P. Mandel, Opt. Commun. **76**, 178 (1990).
[5] O. Benson, G. Raithel, and H. Walther, Phys. Rev. Lett. **72**, 3506 (1994).
[6] M. Dagenais, Z. Pan, T. Ding, and H. Lin, in *Digital Optical Computing, Critical Reviews of Optical Science and Technology,* edited by R. A. Athale (SPIE, Bellingham, WA, 1990), p. 126.
[7] R. Lang, IEEE J. Quantum Electron. **QE-18**, 976 (1982).
[8] F. Choa and T. L. Koch, J. Lightwave Technol. **1**, 73 (1991).
[9] R. Hui, S. Benedetto, and I. Montrosset, Opt. Lett. **18**, 287 (1992).
[10] R. Gilmore, *Catastrophe Theory for Scientists and Engineers* (J. Wiley, New York, 1981).
[11] G. Goldsztein *et al.* (to be published).
[12] Other reasonable definitions of the hysteresis loop give the same scaling laws.
[13] P. Jung, G. Gray, R. Roy, and P. Mandel, Phys. Rev. Lett. **65**, 1873 (1990).
[14] W. A. Hamel, Ph.D. thesis, Leiden, 1991, p. 79.
[15] C. N. Luse and A. Zangwill, Phys. Rev. E **50**, 224 (1994), and references therein.